

CHAPTER 14

Tire Data Treatment

"These nondimensional coefficients are the primary language of applications in aerodynamics ... with a small amount of analysis, we have saved a huge amount of effort."

John D. Anderson, Jr.
University of Maryland (Ref. 15)



Introduction

As Anderson notes in the quote above, aerodynamicists have been very successful in reducing voluminous aircraft force and moment test data to nondimensional coefficient form. These coefficients are based on normalization by the dynamic pressure and a characteristic area and length. Thus the coefficients enable the forces/moments to be determined for any vehicle size and operating condition.

Tires on automobiles and wings on aircraft perform similar functions, but until fairly recently automotive engineers have generally represented the results of tire tests in pounds and foot-pounds in look-up tables with interpolation routines.

In this chapter we first discuss some of the problems of obtaining high-quality tire data, then we give an overview of tire data nondimensionalization—an efficient way to handle tire force/moment data for vehicle analysis of race (and production) car handling.

This chapter was written by Dr. Hugo Radt, MRA, the originator of the tire nondimensionalizing technique. Dr. Radt and the authors wish to acknowledge substantial support by Goodyear and Chrysler for the development of the nondimensional technique.

A typical test for forces and moments on a single tire includes variations of slip angle, load, camber angle, and traction/braking at one inflation pressure and speed. Assuming no means for combining or correlating data at different test conditions, a complete test for one tire typically would include 17 values of slip angle at 6 loads, and 5 camber angles. Traction/braking tests are usually performed by sweeping through the longitudinal force while holding the other test conditions fixed; this test schedule would require 510 such traction/braking sweeps. Clearly, this would be too costly and would require the use of many tires because combinations of high slip angle, high load, and large traction or braking forces yield rapid tire wear on the test machine. Problems of repeatability also occur when multiple tires are used to obtain one complete set of data. Furthermore, similar sets of tests would have to be repeated if the front and rear tires on the race car are different and if the effects of tire inflation are critical.

Another problem area is the treatment of tire data so that it can be used in the analysis and simulation of vehicle handling. Tables of raw data can be voluminous and require polynomial or spline fits for interpolation between data points. Accuracy may be lost and "jumps" or "bends" may occur in the resulting plots when a change of longitudinal force occurs. An empirically derived fit to tire data, referred to as the "magic formula," has been successful in matching much of the raw data. However, the parameters (constants) of the fit are difficult to obtain and require cross plotting to obtain effects of more than one variable at a time.

14.1 Tire Data Nondimensionalization

An alternative approach is called *Tire Data Nondimensionalization* because it makes use of ratios of the raw data in such a way that the dimensions of the data are eliminated. For example, dividing the lateral force by the product of friction coefficient times load makes the resulting "normalized lateral force" nondimensional. The major objectives of using these nondimensional or normalized variables are to:

- Reduce test time and cost.
- Produce less wear during testing.
- Improve tire data accuracy by smoothing the data for combined conditions and performing fewer tire changes during testing.
- Provide simple, accurate representations of tire data for vehicle simulations.
- Allow potential for including variations of surface friction.
- Provide for straightforward and accurate interpolation of data between loads and potential for extrapolating the data to higher or lower loads than those used during the test program.

- Allow for comparison of the purely nonlinear behavior of different tires or the same tire under different operating conditions.

The approach used in tire data nondimensionalization is to:

1. Combine tire lateral force vs. slip angle data, as functions of load, into single curves for all loads in the range from near zero load to twice the tire rated load or to the maximum load expected during racing. Similarly combine data on self-aligning torque and overturning moment for different loads.
2. Combine slip and camber angles into one effective camber/slip variable, for small camber angles (up to about $\pm 10^\circ$). **Note:** In this chapter, camber angle is used interchangeably with inclination angle (see Figure 2.33 for the strict definitions).
3. Combine slip ratio for traction/braking with slip angle and camber angle to provide one effective resultant slip variable.

14.2 Pure Slip Characteristics

Pure slip characteristics refer to lateral force, self-aligning torque, and overturning moment as functions of load and one of either slip angle or camber angle. Also included are longitudinal force (traction/braking) as a function of load and longitudinal slip ratio.

Slip Angle and Load

Several semi-empirical theories of tire mechanics yield the following relations between dimensionless force and slip angle and between dimensionless self-aligning torque or overturning moment and slip angle.

The nondimensional or normalized lateral force, \bar{F} , is defined by

$$\bar{F} = \frac{F_y}{\mu_y Z} \quad (14.1)$$

Similarly, nondimensional or normalized self-aligning torque, \bar{M}_z , is

$$\bar{M}_z = \frac{M_z}{T_z \mu_y Z} \quad (14.2)$$

and the normalized overturning moment, \bar{M}_x , is

$$\bar{M}_x = \frac{M_x}{P_x \mu_y Z} \quad (14.3)$$

while a normalized slip angle is defined as

$$\bar{\alpha} = \frac{C \tan \alpha}{\mu_y Z} \quad (14.4)$$

That is, \bar{F} , \bar{M}_z , and \bar{M}_x are each functions of $\bar{\alpha}$, independent of the load, because load, Z , is already included in the above relations as well as in determining the (lateral) friction coefficient, μ_y , cornering stiffness, C , pneumatic trail, T_z , and overturning trail, P_x .

Pneumatic trail is the ratio of self-aligning torque to lateral force for small slip angles, while overturning trail is the ratio of overturning moment to lateral force, again for small slip angles. The reasoning behind selection of these particular dimensionless forces and moments and the normalized slip angle is provided in Ref. 124, which discusses several semi-empirical theories.

Before normalizing and plotting tire data, we first take an average of lateral forces between positive and negative slip angles, taking into account the fact that the direction (sign) of the lateral force changes when slip angle changes sign. This averaging process eliminates the values of lateral force at zero slip angle caused by tire asymmetries called *conicity* and *ply steer*. A similar averaging is done for self-aligning torque and overturning moment. Conicity and ply steer effects can be reintroduced, for small slip angles, when performing calculations using nondimensional data fits, but are really of little interest for the race car where one is more concerned about high slip angle behavior.

Figures 14.1 and 14.2 show data points at five different loads, for \bar{F} vs. $\bar{\alpha}$ and \bar{M}_z vs. $\bar{\alpha}$, respectively, for a P195/70R-14 tire. All the data points fall close to the solid curve. This solid curve was generated using the "magic formula" of Refs. 16, 17, and 114, although other mathematical curve fitting techniques such as polynomials could have been used. As an example, the normalized lateral force, \bar{F} , as a function of the normalized slip angle, $\bar{\alpha}$, is represented by the "magic formula" as follows:

$$\bar{F} = D' \sin \theta \quad (14.5)$$

$$\theta = C' \arctan(B' \phi) \quad (14.6)$$

$$\phi = (1 - E')\bar{\alpha} + (E'/B') \arctan(B'\bar{\alpha}) \quad (14.7)$$

The parameters for the solid curve in Figure 14.1 are $B' = 0.714$, $C' = 1.40$, $D' = 1.00$, and $E' = -0.20$.

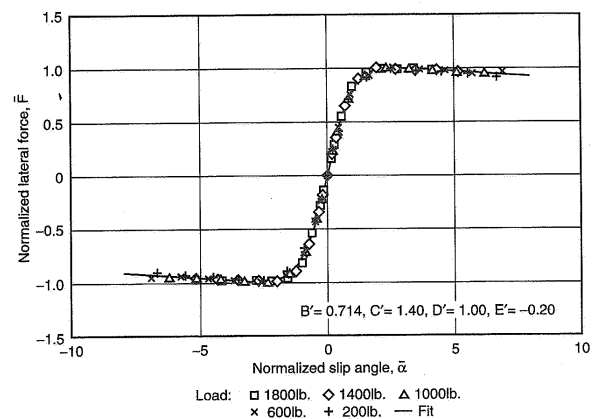


Figure 14.1 Normalized lateral force, 0° camber.

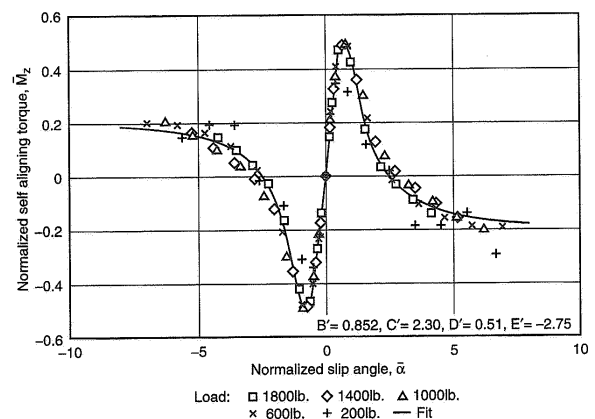


Figure 14.2 Normalized self-aligning torque, 0° camber.

Camber Angle and Load

When camber angle, γ , is varied at zero slip angle, one defines a normalized camber angle, $\bar{\gamma}$, as

$$\bar{\gamma} = \frac{G \sin \gamma}{\mu_y Z} \quad (14.8)$$

where G is the camber stiffness or ratio of camber thrust to camber angle.

Now \bar{F} , \bar{M}_z , and \bar{M}_x are functions of the normalized camber angle, $\bar{\gamma}$. Figure 14.3 shows normalized camber thrust vs. normalized camber angle for all five loads using the square symbol. Data points fall close to the line $\bar{F} = \bar{\gamma}$. (Data exaggerated by scales used in plot.)

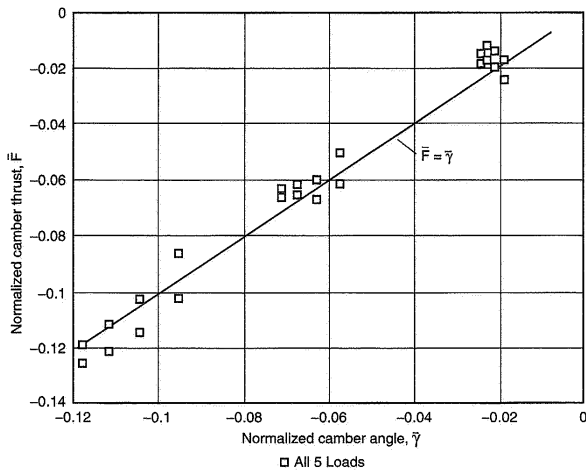


Figure 14.3 Normalized camber thrust, 0° slip angle.

Slip Ratio and Load

For the case of pure traction or braking, but zero slip and camber angles, one defines a normalized longitudinal force, \bar{F}_x , as

$$\bar{F}_x = \frac{F_x}{\mu_x Z} \quad (14.9)$$

and a normalized slip ratio, \bar{S} , as

$$\bar{S} = \frac{k_x S}{\mu_x Z} \quad (14.10)$$

where F_x is the traction or braking force
 k_x is the initial slope of longitudinal force with slip ratio
 μ_x is the longitudinal friction coefficient
 S is the SAE definition of the slip ratio, given by

$$S = \frac{\Omega R_0 - V \cos \alpha}{V \cos \alpha} \quad (14.11)$$

where Ω is the wheel angular velocity (radians per second)
 V is the forward speed of the axle
 R_0 is the rolling radius for free rolling at zero slip angle

For zero slip angle, Eq. (14.11) becomes

$$S = \frac{\Omega R_0}{V} - 1 \quad (14.12)$$

Included in the above definitions is the fact that friction coefficients may differ in the lateral and longitudinal directions.

Figure 14.4 shows data points for the same P195/70R-14 tire for \bar{F}_x as a function of \bar{S} , for five widely varying loads. Again, the points fall close to a single curve which, in fact, represents the same exact equation used to fit the nondimensional plot of lateral force vs. slip angle. This suggests that, once the data are made dimensionless, "one curve fits all." That is, the same mathematical fit can be used for normalized plots of \bar{F} vs. $\bar{\alpha}$, \bar{F} vs. $\bar{\gamma}$, and \bar{F}_x vs. \bar{S} . As described later in this chapter, this same fit applies to combined slip and camber angles and to the resultant normalized force when both lateral and longitudinal forces occur simultaneously, as for braking or traction in a turn. Thus, there appears to be a universal curve fit to the normalized data (for one tire and inflation pressure) that applies to several different forms of slip or combinations thereof.

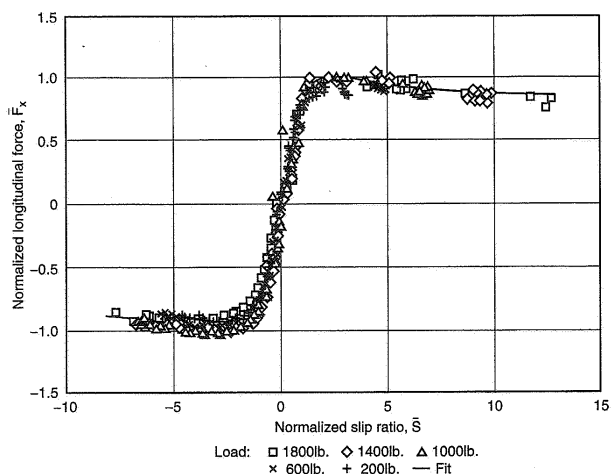


Figure 14.4 Normalized longitudinal force, 0° slip angle.

14.3 Combined Slip Characteristics

Slip and Camber Angles

When slip and camber angles occur simultaneously, we define a new combined slip/camber angle, $\bar{\beta}$, for positive camber angles:

$$\bar{\beta} = \frac{\bar{\alpha}}{1 - \bar{\gamma} \operatorname{sgn} \alpha} \quad (14.13)$$

where $\operatorname{sgn} \alpha$ means the algebraic sign of the slip angle, α . In addition, we introduce a new dimensionless lateral force, FN, again for positive camber angles ($\bar{\gamma} > 0$):

$$FN = \frac{\bar{F} - \bar{\gamma}}{1 - \bar{\gamma} \operatorname{sgn} \alpha} \quad (14.14)$$

FN reduces to \bar{F} of Eq. (14.1) for zero camber angle ($\bar{\gamma} = 0$). Now FN is a function of $\bar{\beta}$, independent of load. When the slip angle is zero, $\bar{\beta}$ is zero, FN is zero and Eq. (14.14)

reduces to $\bar{F} = \bar{\gamma}$, as indicated by the straight line in Figure 14.3. Before calculating and plotting normalized lateral force for combined slip and camber angles, we make use of the following relations for a perfect tire without conicity and ply steer effects:

$$F_y(\alpha, \gamma) \equiv -F_y(-\alpha, -\gamma)$$

$$F_y(-\alpha, \gamma) \equiv -F_y(\alpha, -\gamma)$$

That is, in the absence of conicity and ply steer, positive slip and camber angles yield the same lateral force as for the corresponding negative angles, except for a change of sign.

Figure 14.5 is a plot of the revised definition of dimensionless lateral force, FN, vs. normalized combined slip/camber angle, $\bar{\beta}$, for four different camber angles (0°, -2°, -6°, and -10°) at a load of 1800 lb. Figure 14.6 is a similar plot, but for five different loads and a camber angle of -6°. In both cases the data points fall close to a single (solid) curve, which is the same curve as shown in Figures 14.1 and 14.4.

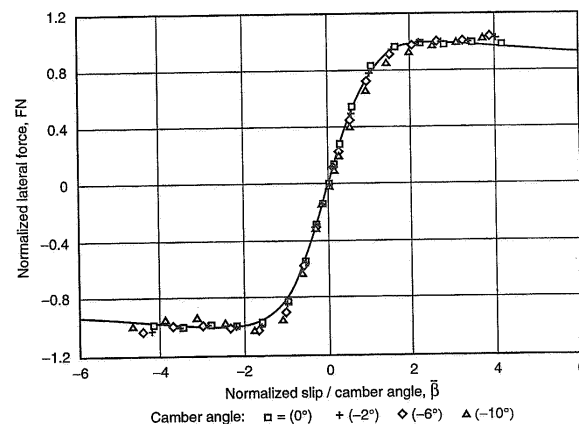


Figure 14.5 Normalized lateral force at 1800 lb. load.

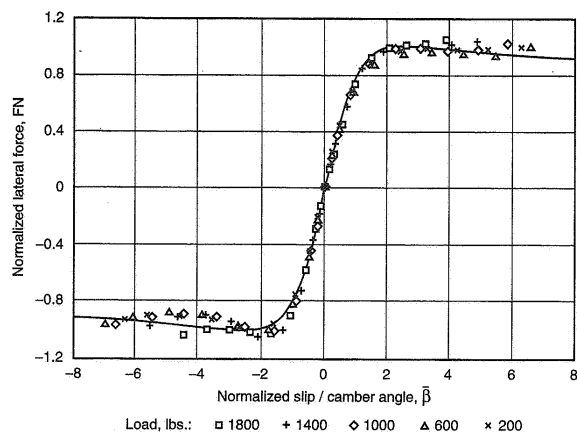


Figure 14.6 Normalized lateral force at -6° camber.

Slip Ratio and Slip Angle

When traction or braking occur in a turn, the tire develops a slip angle due to turning and a slip ratio caused by the longitudinal force. Hence we need a combined normalized slip variable:

$$k = \sqrt{S^2 + \alpha^2} \quad (14.15)$$

and a normalized "resultant" force:

$$R = \sqrt{\bar{F}^2 + \bar{F}_x^2} \quad (14.16)$$

which is found to be a function of k : $R = R(k)$, independent of load.

These definitions are sufficient to make plots of R vs. k , but would be useful only if we could calculate \bar{F} and \bar{F}_x once we have R . To do so we need another relationship obtained from analysis of measured data:

$$\bar{F}S = \eta(k)\bar{F}_x \tan \alpha \quad (14.17)$$

The multiplier $\eta(k)$ is necessary to make Eq. (14.17) hold for both small and large slip angles and slip ratios. The $\eta(k)$ function is of the form:

$$\eta(k) = \begin{cases} \frac{1}{2}[1 + \eta_0] - \frac{1}{2}[1 - \eta_0] \cos(\frac{k}{2}) & |k| \leq 2\pi \\ 1 & |k| > 2\pi \end{cases} \quad (14.18)$$

For small k (i.e., small slip angle and small slip ratio), η is equal to η_0 , whereas for large k , η is 1.

η_0 is determined from the cornering stiffness, C , longitudinal stiffness, k_x , and lateral and longitudinal friction coefficients:

$$\eta_0 = \frac{C\mu_x}{k_x\mu_y} \quad (14.19)$$

Substitution of η_0 from Eq. (14.19) into (14.17), for small k , using the definitions from Eqs. (14.1) and (14.9) and rearranging, shows that:

$$\frac{F_y}{C \tan \alpha} = \frac{F_x}{k_x S}$$

Now, for small slip angles, $F_y = C \tan \alpha$, and for small slip ratios, $F_x = k_x S$. Hence both sides of the above equation are equal to 1 for small slip angles and small slip ratios.

Using Eq. (14.17) along with (14.16), one can separate the nondimensional lateral and longitudinal forces as follows:

$$\bar{F} = \eta(k)R(k) \left[\frac{\tan \alpha}{\sqrt{S^2 + \eta^2 \tan^2 \alpha}} \right] \quad (14.20)$$

$$\bar{F}_x = R(k) \left[\frac{S}{\sqrt{S^2 + \eta^2 \tan^2 \alpha}} \right] \quad (14.21)$$

In Figure 14.7 we have plotted R vs. k for slip angles varying from 1° to 28° , for a single load of 1000 lb. Again, the data points fall close to the solid curve calculated according to Eqs. (14.5) through (14.7) and with the same parameters B' , C' , D' , and E' as used for the normalized lateral force vs. normalized slip angle (Figure 14.1), or normalized combined slip/camber angle (Figure 14.5). Although not shown, the same result, i.e., fitting of the data with the same curve, occurred for other loads.

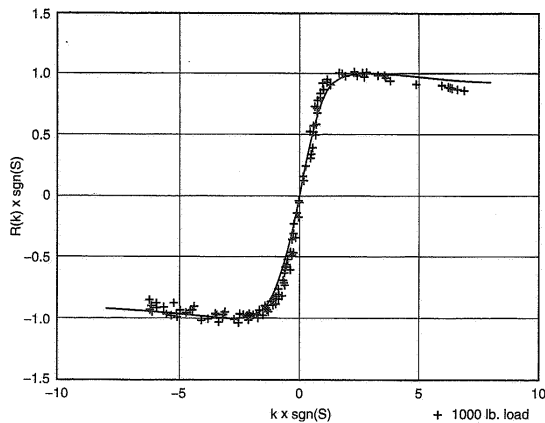


Figure 14.7 Normalized resultant force vs. normalized slip variable.

Once one has obtained a mathematical fit $R(k)$ as indicated, one can reexpand or reconstruct values of lateral and longitudinal force using Eqs. (14.20) and (14.21). This was done and the results plotted in Figure 14.8 for a load of 1000 lb. Raw data points are also plotted for comparison for slip angles of 1° , 2° , and 4° . Similar plotted comparisons are presented in Figure 14.9 for higher slip angles. These comparisons indicate that fitting of the normalized curves for multiple loads and combined cornering and traction/braking faithfully reproduce the original data while providing a compact yet relatively simple way to represent a volume of data.

14.4 Summary of Nondimensionalization of Tire Force/Moment Data

An extensive test program was run on a group of P195/70R-14 tires, including combined effects of slip angle, camber angle and load; slip angle, traction/braking and load. Data from these tests were "normalized" by methods derived from semi-empirical theories attributed to several different authors. The resulting nondimensional graphs indicate that data at different loads can be plotted so as to fall on top of each other. This is referred to as *data compression* because points at different loads nearly compress to a single curve.

In addition, it was found that slip angle and camber angle could be combined into one normalized combined angle and used as the independent variable for the functional

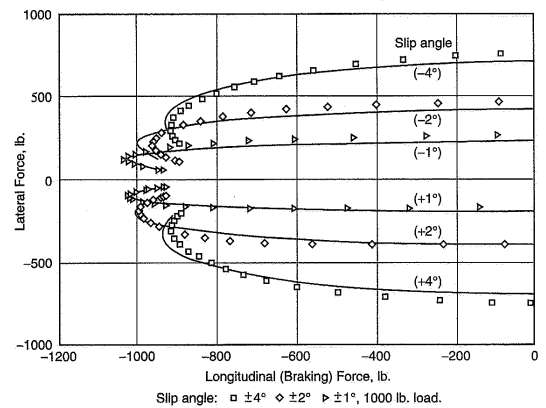


Figure 14.8 Lateral force vs. braking force, constant slip angles.

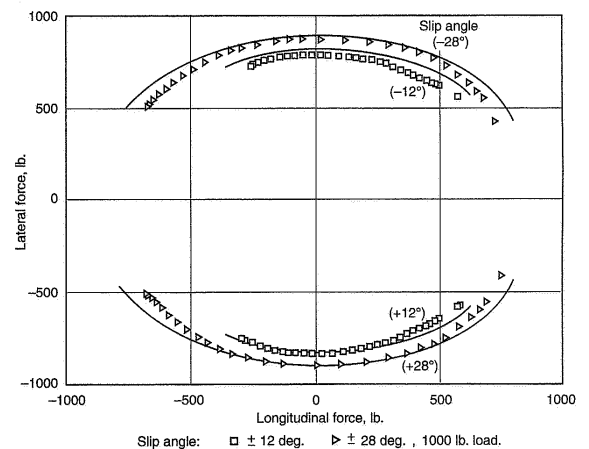


Figure 14.9 Lateral vs. longitudinal force, constant slip angles.

dependence of normalized lateral force that includes camber thrust. The single, normalized curve thus obtained is universal in the sense that it applies for one tire and inflation pressure, over the range of vertical loads, to cases of pure slip angle, pure camber angle, or combinations thereof.

A concurrence of several theories on combined lateral and longitudinal forces led to development of an approach with normalized resultant force as a function of a normalized resultant slip parameter. This function is universal in the sense that it is independent of load and applies equally well to pure slip angle (free rolling), pure traction/braking (zero slip angle), or combinations thereof. Once this function is defined, lateral and longitudinal forces can be obtained knowing slip ratio and slip angle. Essentially, by proper normalization of the data, one need determine only one normalized force function that applies to combinations of slip/camber angle vs. load and slip angle / slip ratio vs. load.

If tire data nondimensionalization and the resulting compression of data is found to be universally valid after further testing of race tires, then a major reduction in test duration can be achieved. Included with such tests are measurements to find the necessary slopes and friction ratios. Such a test program would consist of the following:

- Measurements, at small slip angle, at several loads, to obtain cornering stiffness, pneumatic trail, and overturning trail.
- Measurements at small camber angles, but at zero slip angle, to obtain camber stiffness, camber pneumatic trail, and camber overturning trail (several loads).
- Measurements at one or two high slip angles, at zero camber angle, and several loads to obtain lateral friction coefficients.
- Measurements with zero camber and slip angles, but with small slip ratios to obtain the longitudinal stiffness (slope of longitudinal force with slip ratio). Also, measurements with higher slip ratios to obtain longitudinal friction coefficient at several loads.
- Measurement of the complete cornering curve with slip angle at one intermediate load, zero camber angle, and free rolling.

The burden of effort is then placed on data reduction to determine slopes, normalize the data, fit the normalized data with mathematical functions, and then "reexpand" the forces and moments for varying load, slip angle, slip ratio, and camber angle.

In conclusion, a major problem with the use of vehicle computer models is the difficulty of obtaining consistent and believable tire data. Force/moment data must cover the full range of load, slip angle, camber, and traction/braking. Test facilities for measuring force/moment data suitable for race application are few and even those have operational limits. The nondimensional approach attempts to make up for the deficiencies of experimental data. Of particular importance to racing is the ability to adjust the data for other

friction coefficients in a fundamentally correct manner. The nondimensional approach provides a simple mechanism for varying friction coefficient. Furthermore, it rests on a substantial theoretical base.